Faults and stratigraphic boundaries control evolution of the huge debris flows along the Jinjiang River, China

Zhuoya Liu*, Yi Wen, Xianyin Mao, Qianyong Lv and Guisen Zeng

Electrical Science Institute of Guizhou Power Grid Co., Ltd., China Southern Power Grid, Guiyang, Guizhou, China

This paper investigates the controlling factors of the evolution of debris flows along the Jinjiang River, which is located in an active orogen. The debris flows along the Jinjiang River are threatening nomads and pastures, as well as the power station on the river and its workers. Remote sensing images, geological maps, and field investigations were conducted to determine the distribution of the lithologies, faults, and debris flows. A total of 82.2 km of riverbank and 108 debris flows, including 22 huge flows, were investigated. The results indicate that the distribution of the huge debris flows is primarily controlled by either faults or boundaries between the sedimentary rocks and basalt. Both the faults and the stratigraphic boundaries play crucial roles in the evolution of the huge debris flows along the river. The fractured zone of faults and stratigraphic boundaries provides loose resource materials for the debris flows and is a weak strip prone to incision to become a debris flow valley. However, the lithology has relatively less impact on the evolution of the huge debris flows.

1 Introduction

A debris flow is a mixture of water and particles driven down a slope by gravity. Factors influencing the evolution and distribution of debris flow are of great importance for its forecasting, early warning, prevention, and hazard assessment. Previous studies have indicated that abundant water and an adequate debris supply, land use, disturbed landscape, wildfire, geology, topography, bedrock strength, meteorology, and human economic activities have great effects on the evolution of debris flow (e.g., Lorente et al., 2002; Wieczorek et al., 2004; Larsen et al., 2006; Picarelli et al., 2008; Wei et al., 2008; Klubertanz et al., 2009; Riley et al., 2013; Wei et al., 2017; Li et al., 2021; Xiong, 2023).

The Pamir and Tibetan Plateaus are in the active Himalayan–Tibetan orogen in central Asia (Yuan et al., 2013). They were formed due to the collision between the Indian Plate and Eurasia since the early Cenozoic (Ding et al., 2016; Hu et al., 2017). Debris flow is one of the main geohazards in this area (Alford et al., 2000; Shroder et al., 2011; Khan, 2013; Zhang et al., 2014; Deng et al., 2017; Huang et al., 2017; Li et al., 2018; Mohanty et al., 2018; Wei et al., 2018; Yuan et al., 2018; Lin et al., 2023; Zhang T.T et al., 2023), where there are Alpine landscape, active faults, and strongly metamorphosed rocks, glaciers, and extreme weather

FIGURE 1
Location map of the study area.

([Brookfield, 2008](#); [Fuchs and Gloaguen, 2013](#); [Schoenbohm et al., 2014](#); [Owczarek et al., 2017](#)). Debris flow is threatening local people's lives and properties. However, due to the tough natural and, sometimes, social and economic environments, research on the debris flows in the Pamir and Tibetan Plateaus is limited compared to those in other mountainous areas such as the Alps ([Hurlimann et al., 2003](#); [Pirulli and Marco, 2010](#); [Toreti et al., 2013](#); [Nikolopoulos et al., 2015](#); [Dietrich and Krautblatter, 2017](#); [Lei et al., 2022](#); [Du et al., 2023](#); [Zhang M.Z et al., 2023](#)).

In this study, we select the Jinjiang River in Wuqia, Xinjiang Uygur Autonomous Region, China ([Figure 1](#)), as a pilot case study to investigate the factors that control the evolution of debris flows along the river, which is very important for remote areas where debris flow research is limited. The conclusions can guide debris flow monitoring and early warning and local pasture planning and construction. The Jinjiang River is located in northern Pamir Plateau, and it is dominated by active faults, tectonic movements, and high-density debris flows and contains multiple lithologies such as volcanic, sedimentary, and metamorphic rocks. It provides an excellent benchmark for studying the factors controlling the distribution of debris flow in an active orogen.

2 Geological setting

The Jinjiang River is located near the boundary between Kyrgyzstan and China and is the merger of the Suyueke River and Tulugart River, which originate from the west Tienshan range and merge together at Tuoyun town ([Figure 1](#); [Figure 2](#)). The river is situated in the Tienshan Orogen, which extends roughly in the EW

direction and has been uplifting since the collision between the Indian Plate and Eurasia Plate.

A series of roughly EW-direction faults and folds were formed in the Tienshan Orogen due to the SN compression from the Indian Plate. The Jinjiang River is cut across by the large Maidan fault ([Figure 2](#)). Many small subsidiary faults developed, parallel or perpendicular to the Jinjiang River. Earthquakes occur frequently in the study area. There have been 17 earthquakes in Wuqia County since 1898, among which 4 earthquakes were between 7 and 8 in magnitude. Especially between 1983 and 1987, there were 3 earthquakes between 6 and 7 in magnitude. The latest earthquake larger than 6.0 in magnitude occurred on 5 October 2008. The magnitude was 6.8 and triggered numerous small-scale landslides and rockfalls in the study area.

The lithology along the investigated segment of the river includes: (1) Sedimentary conglomerate, mudstone, and sandstone, which were formed in the Jurassic, Carboniferous, Cretaceous, Devonian, and Tertiary periods. In particular, the red mudstone and sandstone that formed in the Tertiary period have gone through weak diagenesis and their strength is not developed very well. (2) Metamorphic rocks, including phyllite and slate metamorphosized from mudstone and sandstone. (3) Basalt, which is distributed at the junction of the three rivers and appears in the Tertiary mudstone and sandstone.

The average precipitation in the study area is 230 mm per year, with a maximum value of 326.4 mm and a minimum value of 139 mm. Rainfall and water from snow melt mainly occur from May to August and can reach as much as 60% of the annual precipitation. Short-term heavy rainfall is the main cause of debris flow in this area ([Wang et al., 2020](#)). However, there are

FIGURE 2
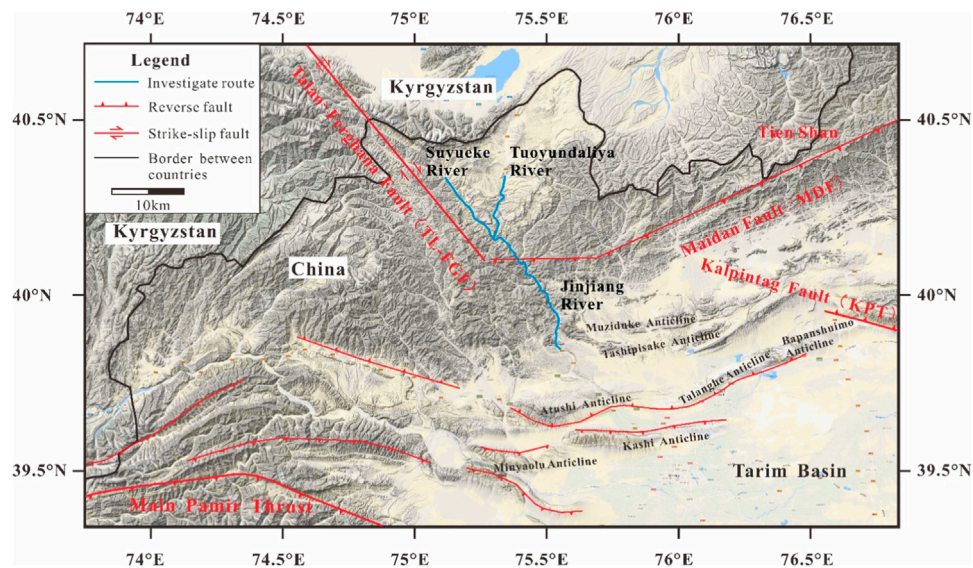Tectonic background of the study area. The figure was drawn based on a 1: 5,000,000 geological map (Chen et al., 2003) and DEM downloaded from Google Earth.
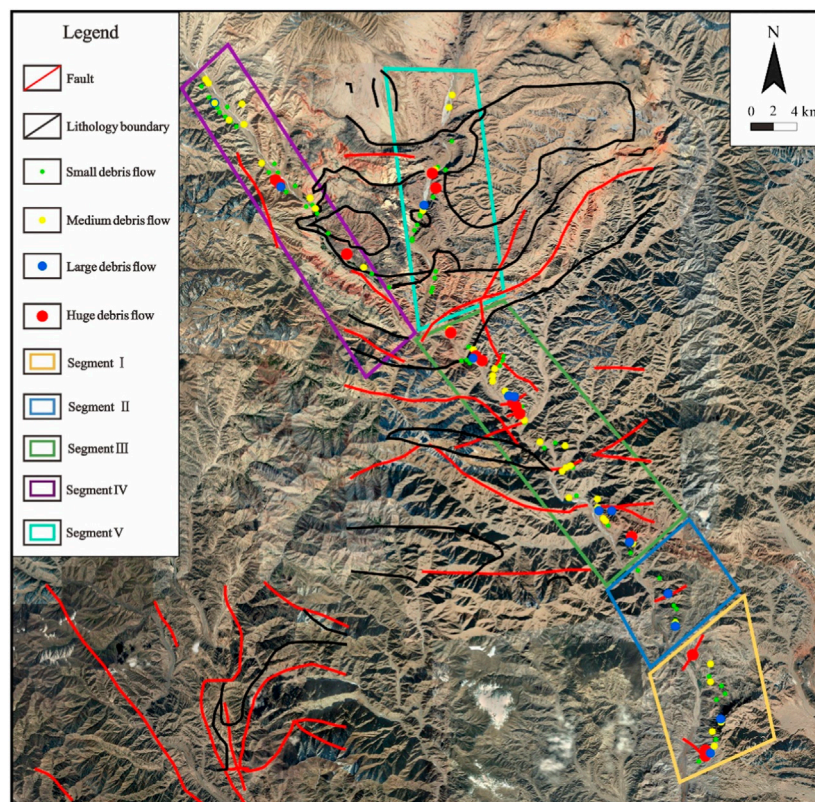

FIGURE 3
Distributions of debris flow, fault, and lithology in the study area. The rectangles represent different segments divided according to the distribution characteristics of the debris flows. The remote sensing image was downloaded from Google Earth.
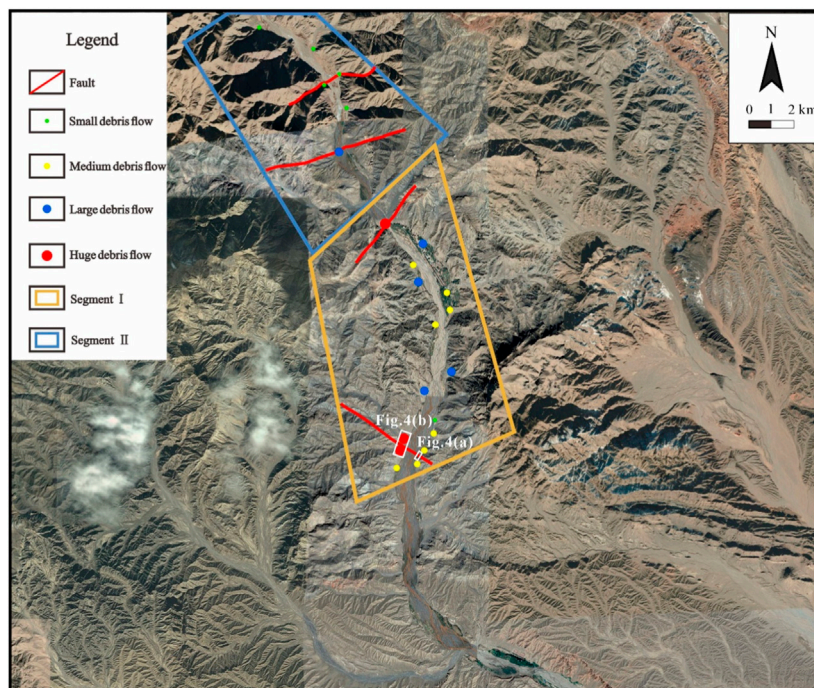
FIGURE 4
Distributions of the debris flows and faults in Segments I and II. The map was downloaded from Google Earth. Because no remote sensing image and large-scale geological map of this segment are available, all the information related to fault, lithology, and debris flow in this map was obtained through field investigation. Lithologies that are not right near the riverbed could not be obtained only through the map and were therefore not marked in this map.
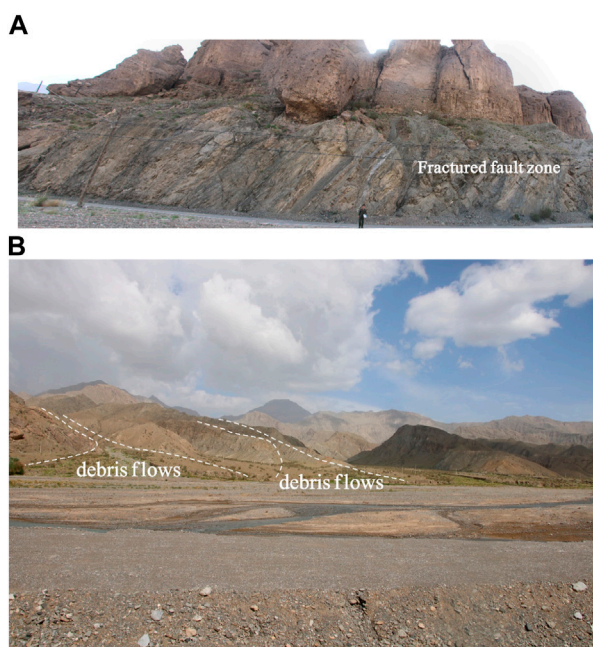

FIGURE 5
Two-hundred-wide fractured fault zone **(A)** and the huge debris flows originated along it at the opposite bank **(B)**.

no detailed data on the precipitation and corresponding rainfall-induced debris flow in the study area due to the adverse natural environment, sparse population, and consequent absence of monitoring stations.

The local people depend mainly on animal husbandry. The Jinjiang River Basin is an important pasture for the local people. In addition, a waterpower station is under construction on the river. Therefore, the debris flows along the Jinjiang River are threatening nomads and pastures, as well as the power station and its workers.

3 Methods

A 1:200,000-scale geological map is available in the study area, but the scale is not large enough and far from satisfactory for our study. The map demonstrates large-scale faults and lithologic distribution, which were used to supplement and calibrate the results from our field investigation and remote sensing image interpretation.

Two remote sensing images with a resolution of 0.8 m taken by the China Aero Geophysical Survey and Remote Sensing Center for Land and Resources in August, 2017, were used to interpret the distributions of debris flows, lithologies, and faults. Since our study area goes beyond the range of the above two remote sensing images, we therefore downloaded another two Google Earth images as
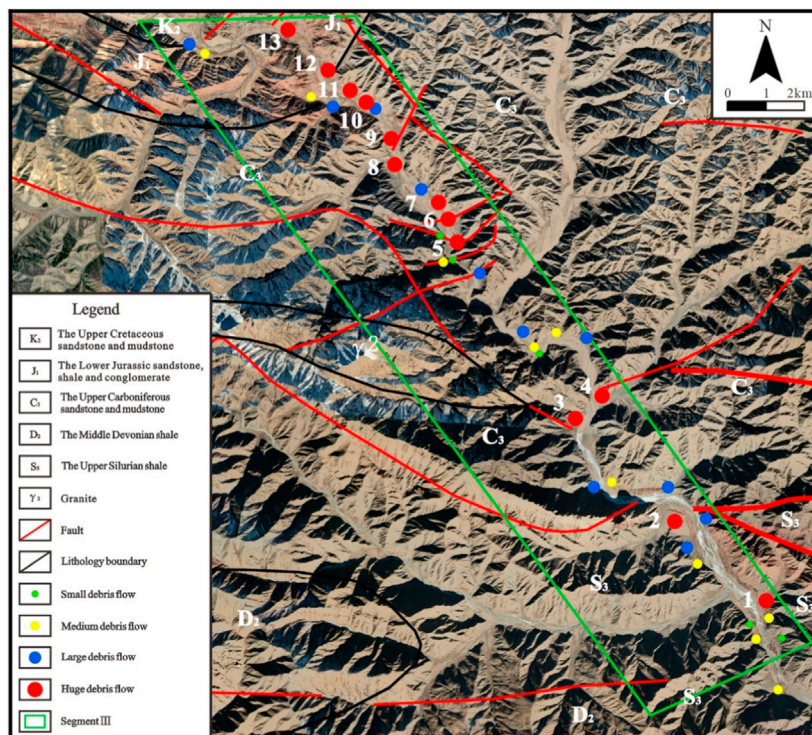
FIGURE 6
Distribution of the debris flows, lithologies, and faults in Segment III. The remote sensing image was taken by the China Aero Geophysical Survey and Remote Sensing Center for Land and Resources in August, 2017. The information related to the debris flows, lithologies and faults in this map was obtained through the geological map, the interpretation of the remote sensing image and the field investigation.

supplements. Although they were not as clear as the remote sensing images, we could also roughly distinguish the debris flows and, in some areas, the lithologies. The interpretation of the above remote sensing images was conducted by the Sichuan Geological Survey.

We conducted field investigations to examine the debris flows, faults, and lithologies in the study area. All the debris flows are distributed along the river valleys. We did not reach every part of every debris flow because it is very hard to access some of them due to the tough natural conditions. However, we made sure that we reached every debris flow deposit to determine their average thickness. For the faults the lithologies that are not distributed along the river, we mainly determined them through the geological map, Google Earth map, and interpretation of the remote sensing images.

All the information obtained was highlighted on the two remote sensing images and two images from Google Earth. Debris flows were marked as solid circles with four different areas based on their volumes. Debris flow with volumes larger than $50\times10^4\,m^3$, $20–50\times10^4\,m^3$, $20–2\times10^4\,m^3$ and smaller than $2\times10^4\,m^3$ were classified as huge, large, medium, and small debris flows, respectively, according to the *Specification for Investigation of Landslides, Rockfall, and Debris Flow 1: 5000 (DD 2008-02)* by the China Geological Survey (2008). Their volume is the volume of deposit, which could be measured using the area obtained from the remote sensing images or the Google Earth map, multiplying the average thickness of the deposit estimated in the field. The structure and composition of a debris flow deposit and alluvial deposit are

obviously different. A debris flow deposit is not sorted by particle size, and the rocks are angular, while an alluvial deposit is well sorted in particle size, and its gravels are well rounded. Furthermore, the lithology of rocks in the above two deposits is always different because they are from different sources. Based on the above differences, we distinguished two deposits and estimated the average thickness of the debris flow deposits.

The distributions of the debris flow and fault along the studied segment of the Jinjiang River are presented in Figure 3, with faults marked as red solid lines and the boundaries between the lithologies marked as black solid lines. To make Figure 3 more readable, the distribution of the lithologies in the studied area is presented in Figure 3; Figure 5; Figure 6; Figure 9, which are its enlarged figures.

4 Distribution of debris flow

The Jinjiang River can be divided into five segments based on the distribution characteristics of the debris flows (Figure 4).

Segment I: This segment is 8.8 km in length (Figure 4). The lithology along the river in this segment includes mainly lightly metamorphosed sandstone and mudstone. Because of the active tectonic movements, the surface of the rocks is very fractured. There are a total of 16 debris flows in this segment, of which 13 are less than $50\times10^4\,m^3$, distributed in the fractured rocks without fault, including 5 large and 8 medium ones. Three huge flows are distributed along the two faults in this segment.
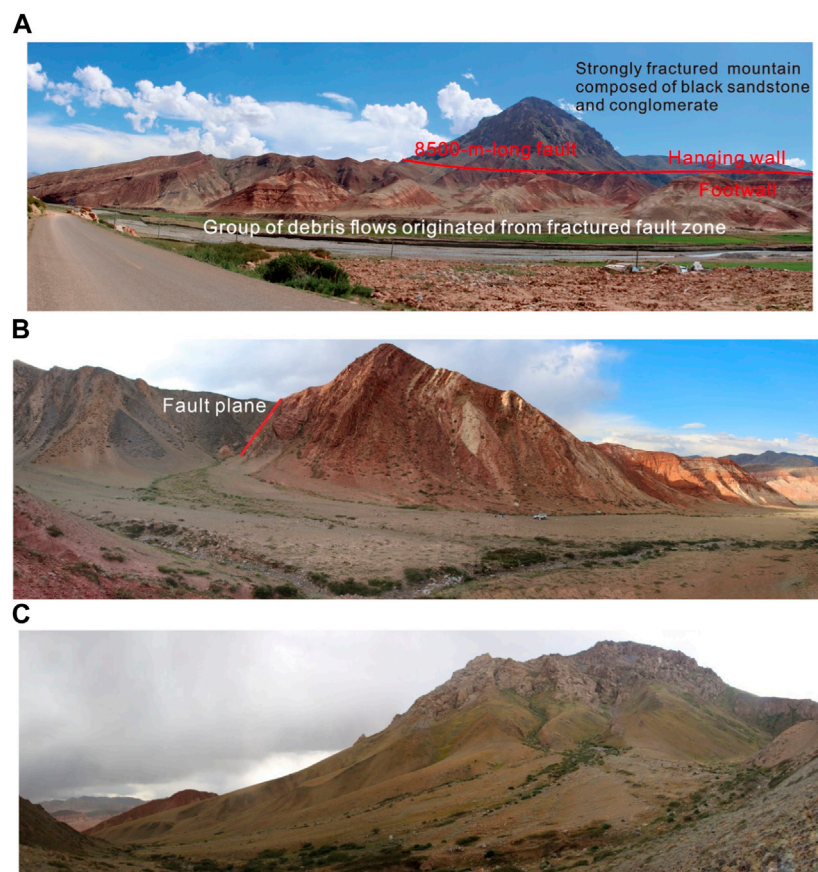
FIGURE 7
A group of debris flows originated from the strongly fractured fault zone. **(A)** The strongly fractured black sandstone and conglomerate in the hanging wall could be seen from the opposite bank. The mountains in the following **(B, C)** are the lateral banks of one of the debris flow valleys. **(B)** The fault plane in the left mountain of one of the debris flow valleys. The hanging wall is black sandstone and conglomerate. The footwall is red mudstone and sandstone. **(C)** The opposite bank of the mountain in **(B)**. The black sandstone and conglomerate in the hanging wall near the fault plane is strongly fractured (The fractured mountain seen in **(A)**). The deposits of rockfalls and landslides occurred in the hanging wall accumulated at the slope toe, becoming the material resource of debris flow.

Figure 5 displays the fractured fault zone of about 200 m wide (at the south end of the investigated route) on the west bank of the river and the debris flows in the fault zone on the opposite side of the river.

(a) Cross-section of a fractured fault zone of about 200 m wide on the west bank exposed by slope excavation for road building. The lower part is lightly metamorphosed sandstone and mudstone, where the fractured fault zone exists. The upper part is conglomerate. This indicates that the fault occurred before the conglomerate was formed.
(b) Debris flows in the 200-m-wide fault zone on the east bank of the river.

Segment II: This segment is about 8.4 km long (Figure 4). The lithology includes lightly metamorphosed limestone and mudstone with two faults perpendicular to the river. The rocks are extremely fractured due to the active tectonic movements and strong weathering.

In this segment, only sporadic debris flows, including a huge flow and five medium ones, were developed. The huge debris flow evolved along one of the two faults. The other fault is a smaller one, and two medium debris flows on both sides of the river are distributed along it.

Segment III: This segment is 25 km long (Figure 6). The lithology includes mudstone, sandstone, and lightly metamorphosed mudstone and sandstone. The rocks are more complete than those in Segments I and II. Faults are well developed in this segment. Several large and small faults are distributed roughly parallel or perpendicular to the river.

In this segment, debris flow is particularly intense, with a total of 39 incidents, 13 of which were classified as huge. The huge debris flows were either found along river-parallel faults or originated from river-perpendicular faults. To facilitate the analysis of the relationship between the huge debris flows and the faults, they were numbered from No. 1 to No. 13.

Debris flows No. 1, 2, 3, 7, 8, 10, 11, 12, and 13 incised the river-perpendicular fault zones, and the debris flow deposits reached the riverbed. Debris flows No. 4, 5, 6, and 9 originated from the river-perpendicular fault zones. The representative photo of this kind of debris flow that originated from and perpendicular to the fault zone can be found in Figure 7.
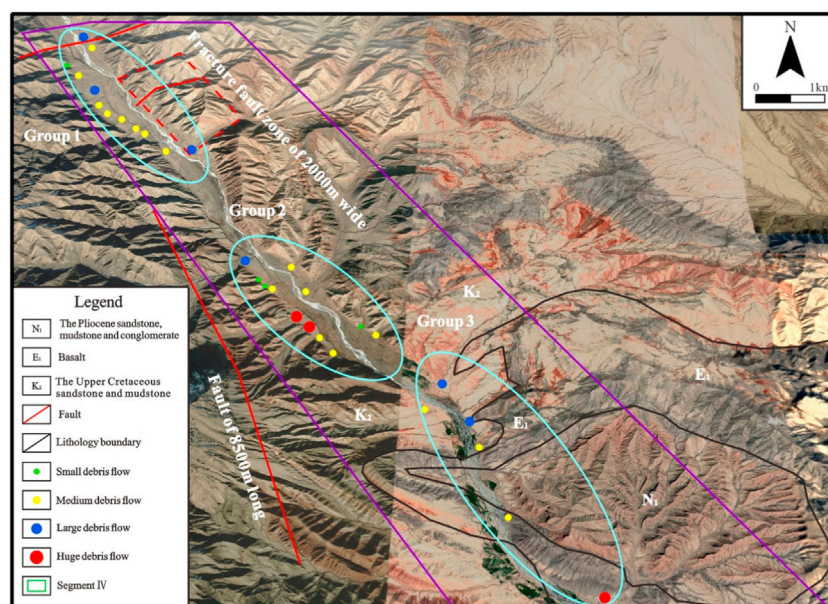
FIGURE 8
Distributions of the debris flows, lithologies, and faults in Segment Ⅳ. This map was downloaded from Google Earth. The information related to lithology, fault, and debris flow was obtained through the geological map, field investigation, and interpretation of the map.
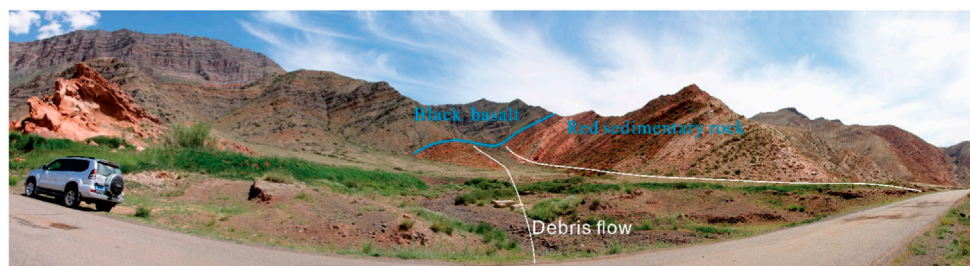

FIGURE 9
Debris flows developed along the interface between the red sedimentary rocks and basalt. The scene is deformed (e.g., the road is almost straight rather than curved) due to the photo-syntheses.

Segment Ⅳ: This segment is 19 km long and is part of the Suyueke River (Figure 8). The lithology along the river mainly includes red mudstone and sandstone, as well as black basalt, which appears at the junction of the three rivers. Although the red mudstone and sandstone are weak in strength because they were formed in the Tertiary and their diagenesis was not very good, they are quite intact. The surface of the basalt is strongly weathered and very fractured, hence comprising cubes with several cubic centimeters in volume. There are three faults in this area. Two faults are perpendicular to the river, and one of them presents an about 2000-m-wide fractured fault zone along the river (Figure 8). The third one is parallel to the river and about 8.5 km long.

(a) A group of debris flows originated from the fractured fault zone. The strongly fractured black sandstone and conglomerate in the hanging wall could be seen from the opposite bank. The

mountains in the following (b) and (c) are the lateral banks of one of the debris flow valleys.

(b) The fault plane on the left mountain of one of the debris flow valleys. The hanging wall is black sandstone and conglomerate. The footwall is red mudstone and sandstone.

(c) The opposite bank of the mountain in (b). The black sandstone and conglomerate on the hanging wall near the fault plane is strongly fractured (the fractured mountain seen in (a)). The deposits of rockfalls and landslides that occurred on the hanging wall accumulated at the foot of the slope, becoming the material resource of the debris flow.

In this segment, there are three groups of debris flows (Figure 8). Group 1 is at the northwest end of our investigated route and contains 12 large, medium, and small debris flows. All the debris flows are controlled by the two faults and their fractured zones, and one of the
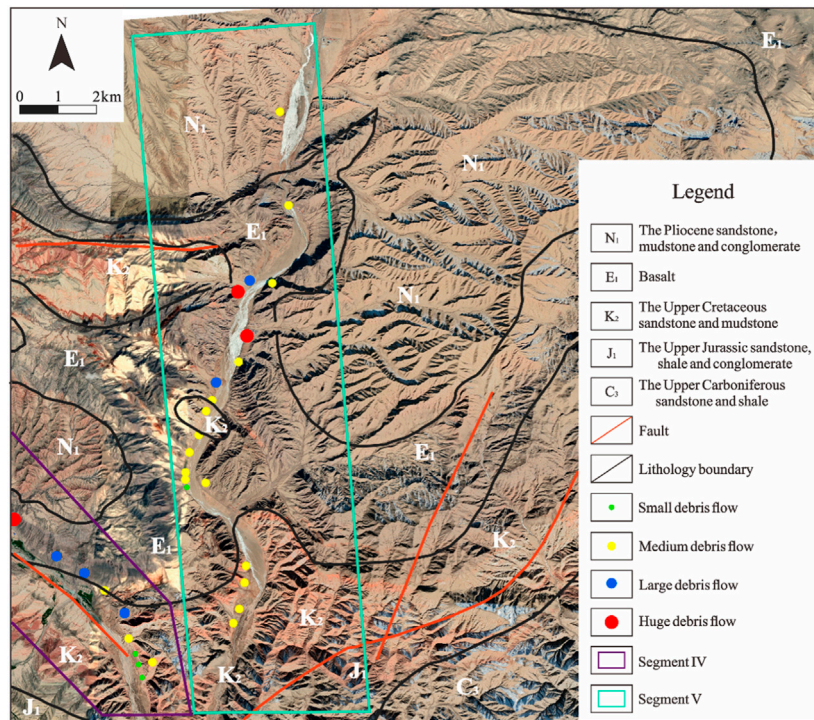
FIGURE 10
Distributions of the debris flows, lithologies, and faults in Segment V. The remote sensing image was taken by the China Aero Geophysical Survey and Remote Sensing Center for Land and Resources in August, 2017. The information related to the debris flows, lithologies, and faults in this map was obtained through the geological map, the interpretation of the remote sensing image, and the field investigation.
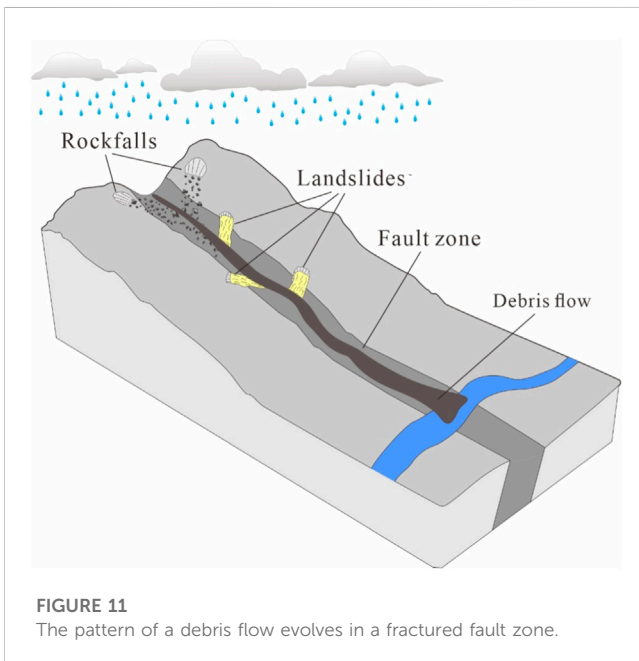

FIGURE 11
The pattern of a debris flow evolves in a fractured fault zone.

fractured zones reaches about 2000 m in width. We investigated the fault zone on the east bank of the river, and therefore, we only drew the fault on this side and inferred that it extends in the same strike to the other side, where most of the debris flows are distributed.

With the exception of four medium and small flows on the east bank, all the debris flows on the west bank in Group 2 are perpendicular to the 8.5-km-long fault, which is roughly parallel to the river (Figure 8). The resource areas of these debris flows are in the fractured zone of the fault, which is between the hanging wall of the black mudstone and sandstone and footwall of red mudstone and sandstone. It is more than 100 m in width. Small-scale landslides and rockfalls frequently occur in fractured rocks of the fault zone. Their debris was deposited at the slope toe in the valley and became the material resources of the debris flow.

There are six debris flows in Group 3, including one huge, two large, and three medium ones. All the three huge and large debris flows evolved along or near the interfaces among the red sedimentary mudstone and sandstone and the black basalt (Figures 9, 10). The rocks in the interface between the sedimentary rocks and basalt are pretty fractured and underwent incision to become debris flow valleys.

Segment V: This segment is about 25 km long (Figure 10). The lithology includes red mudstone and sandstone, as well as black basalt near the junction of the three rivers. The red mudstone and sandstone that formed in the Tertiary is weak in strength but comparatively complete. There is no fault found in this area.

There are a total of 19 debris flows in this segment. Most of them are medium and small and distributed in the red mudstone and sandstone due to their weak strength. Two huge and two large debris flows are distributed near the interface between the sedimentary rocks and the basalt, such as those in Segment IV.

5 Discussion and conclusions

A total of 82.2 km of riverbank and 108 debris flows, including 22 huge flows, were investigated. Almost all the huge debris flows evolved along or originated from the faults or along the interfaces between the sedimentary rocks and basalt. Fault and stratigraphy, therefore, control the distribution of debris flow along the Jinjiang River. In Segment III, the rocks are not strongly weathered and, therefore, are more complete than those in Segments I and II, but the debris flows are well developed and most intense due to widespread faults. While in Segment II even the rocks are strongly weathered and fractured, only sporadic medium debris flows are distributed without faults and an interface between the sedimentary rock and basalt. Furthermore, in Segments IV and V, five huge debris flows either originate from faults or along the boundaries of the sedimentary rocks and basalt. Only medium and small debris flows evolved in the weak sedimentary mudstone and sandstone without faults and strata boundaries. We hence conclude that lithology has little impact on evolution of large-scale debris flows.

Faults have two aspects of effects on the evolution of debris flow (Figure 11). Firstly, a fractured fault zone is prone to incision to become a debris flow valley (He et al., 2003; You et al., 2023). Secondly, landslide and rockfall occur in the fractured rocks of the fault zone and, therefore, provide the loose deposits for the material resources of debris flows (Huang et al., 2022; Jin et al., 2023). For the debris flows that develop along fault, both of the above two effects play important roles during their evolution. For the debris flows that originate from the perpendicular fault zones, only the former effect takes part in their evolution.

Huge debris flows develop along or near the interface between red sedimentary rocks and basalt. This is because the red mudstone and sandstone were compressed and sheared to be strongly fractured by the magma during its eruption. Furthermore, the basalt underwent strong incision to become small cubes, from a few cubic centimeters to more than ten cubic centimeters in volume, by joints produced during the condensation of the magma. Therefore, the fractured zone of about several tens of meters in width, or even more than hundreds of meters in width, along the interface between the two kinds of lithologies could supply loose material and is prone to gradually incision into a valley by rainfalls and debris flows, which are actually the same as the effects of faults.

Debris flow is an important form of erosion and sedimentation of orogens. It is, therefore, very common that debris flows develop well in an orogen (Wang, 2013; Chen et al., 2015). However, there have been few studies on the controlling factors and mechanisms of debris flows in orogens. Many studies related to orogenic erosion and sedimentation have indicated that debris flows occur due to tectonic uplift and rainfall (Savi et al., 2016; Wang et al., 2022) but did not reveal exactly what factors control the evolution of debris flows and how they occur. Our study indicates that the faults and boundaries between sedimentary rocks and basalt control the distribution of debris flows along Jinjiang River in the Himalayan–Tibetan orogen, and it explains their roles in the evolution of debris flows. The conclusions can provide a theoretical basis for the monitoring, early warning, and forecasting of debris flows and construction planning in orogenic belts.

Data availability statement

The original contributions presented in the study are included in the article/Supplementary material, further inquiries can be directed to the corresponding author.

Author contributions

ZL, YW, XM, QL, and GZ contributed to conception and design of the study. ZL dealt the data and wrote the paper, YW, XM, QL, and GZ designed the field investigation route and conducted the field investigation. All authors contributed to the article and approved the submitted version.

Conflict of interest

Authors ZL, YW, XM, QL, and GZ were employed by Electrical Science Institute of Guizhou Power Grid Co., Ltd.

Publisher's note

All claims expressed in this article are solely those of the authors and do not necessarily represent those of their affiliated organizations, or those of the publisher, the editors and the reviewers. Any product that may be evaluated in this article, or claim that may be made by its manufacturer, is not guaranteed or endorsed by the publisher.

References

Alford, D., Cunha, S. F., and Ives, J. D. (2000). Lake sarez, Pamir mountains, Tajikistan: Mountain hazards and development assistance. *Mt. Res. Dev.* 20, 20–23. doi:10.1659/0276-4741(2000)020[0020:lspmtm]2.0.co;2

Brookfield, M. E. (2008). Evolution of the great river systems of southern Asia during the Cenozoic India-Asia collision: Rivers draining north from the Pamir syntaxis. *Geomorphology* 100, 296–311. doi:10.1016/j.geomorph.2008.01.003

Chen, Y., Gen, S., Xie, L., Ding, X., Fu, D., Wu, L., et al. (2003). *1: 5,000,000 geological map of China*. Second Edition.

Chen, Y., Shyu, J. B. H., and Chang, C. (2015). Neotectonic characteristics along the eastern flank of the Central Range in the active Taiwan orogen inferred from fluvial channel morphology. *Tectonics* 34, 2249–2270. doi:10.1002/2014tc003795

Deng, M., Chen, N., and Liu, M. (2017). Meteorological factors driving glacial till variation and the associated periglacial debris flows in Tianmo Valley, south-eastern Tibetan Plateau. *Nat. Hazards Earth Syst. Sci.* 17, 345–356. doi:10.5194/nhess-17-345-2017

Dietrich, A., and Krautblatter, M. (2017). Evidence for enhanced debris-flow activity in the northern calcareous Alps since the 1980s (plansee, Austria). *Geomorphology* 287, 144–158. doi:10.1016/j.geomorph.2016.01.013

Ding, L., Qasim, M., Jadoon, I. A. K., Khan, M. A., Xu, Q., Cai, F., et al. (2016). The India-Asia collision in north Pakistan: Insight from the U-Pb detrital zircon provenance of Cenozoic foreland basin. *Earth Planet. Sci. Lett.* 455, 49–61. doi:10.1016/j.epsl.2016.09.003

Du, J., Zhang, H. Y., Hu, K. H., Wang, L., and Dong, L. Y. (2023). Prediction of the periglacial debris flow in southeast tibet based on imbalanced small sample data. *Water* 15 (2), 310. doi:10.3390/w15020310

Fuchs, M. C., and Gloaguen, R. (2013). Tectonic and climatic forcing on the rivers in Pamir. *Int. J. Earth Sci.* 102, 2005–2006. doi:10.1007/s00531-013-0929-x

He, N., Song, Y. B., Hu, G. S., Yang, Z. Q., Fu, Q. X., and Gurkalo, F. (2023). The distribution law and coupling factor of debris flows in the G318 Linzhi-Lhasa section of the Sichuan-Tibet traffic corridor. *Front. Ecol. Evol.* 11, 1166239. doi:10.3389/fevo.2023.1166239

Hu, X., Wang, J., Wei, A., Garzanti, A., and Li, J. (2017). Constraining the timing of the India-Asia continental collision by the sedimentary record. *Sci. China Earth Sci.* 60 (4), 603–625. doi:10.1007/s11430-016-9003-6

Huang, H., Wang, Y. S., Li, Y. M., Zhou, Y., and Zeng, Z. Q. (2022). Debris flow susceptibility assessment in China: A comparison between traditional statistical and machine learning methods. *Remote Sens.* 14 (18), 4475. doi:10.3390/rs14184475

Huang, X., Li, Z., Yu, D., Xu, Q., Fan, J., Hao, Z., et al. (2017). Evolution of a giant debris flow in the transitional mountainous region between the Tibetan Plateau and the Qinling Mountain range, Western China: Constraints from broadband seismic records. *J. Asian Earth Sci.* 148, 181–191. doi:10.1016/j.jseaes.2017.08.031

Hurlimann, M., Rickenmann, D., and Graf, C. (2003). Field and monitoring data of debris-flow events in the Swiss Alps. *Can. Geotechnical J.* 40, 161–175. doi:10.1139/t02-087

Jin, W., Cui, P., Zhang, G. T., Wang, J., Zhang, Y. X., and Zhang, P. (2023). Evaluating the post-earthquake landslides sediment supply capacity for debris flows. *Catena* 220, 106649. doi:10.1016/j.catena.2022.106649

Klubertanz, G., Laloui, L., and Vulliet, L. (2009). Identification of mechanisms for landslide type initiation of debris flows. *Eng. Geol.* 109, 114–123. doi:10.1016/j.enggeo.2009.06.007

Larsen, I. J., Pederson, J. L., and Schmidt, J. C. (2006). Geologic versus wildfire controls on hillslope processes and debris flow initiation in the Green River canyons of Dinosaur National Monument. *Geomorphology* 81, 114–127. doi:10.1016/j.geomorph.2006.04.002

Lei, Y., Gu, H. H., and Cui, P. (2022). Vulnerability assessment for buildings exposed to torrential hazards at Sichuan-Tibet transportation corridor. *Eng. Geol.* 308, 106803. doi:10.1016/j.enggeo.2022.106803

Li, S., Armitage, S. J., Stevens, T., and Meng, X. (2018). Alluvial fan aggradation/incision history of the eastern Tibetan plateau margin and implications for debris flow/debris-charged flood hazard. *Geomorphology* 318, 203–216. doi:10.1016/j.geomorph.2018.06.016

Li, Y. J., Meng, X. M., Guo, P., Dijkstra, T., Zhao, Y., Chen, G., et al. (2021). Constructing rainfall thresholds for debris flow initiation based on critical discharge and S-hydrograph. *Eng. Geol.* 280, 105962. doi:10.1016/j.enggeo.2020.105962

Lin, M. A., Gong, C., Huang, H., and Yang, D. X. (2023). Damage model and the influence factors of mitigation engineering against glacial debris flow in the parlung River Basin, SE Tibetan plateau. *Water* 15 (6), 1098. doi:10.3390/w15061098

Lorente, A., Garcia-Ruiz, J. M., Begueria, S., and Arnaez, J. (2002). Factors explaining the spatial distribution of Hillslope debris flows. *Mt. Res. Dev.* 22, 32–39. doi:10.1659/0276-4741(2002)022[0032:fetsdo]2.0.co;2

Mohanty, A., Hussain, M., Mishra, M., Kattel, D. B., and Pal, I. (2018). Exploring community resilience and early warning solution for flash floods, debris flow and landslides in conflict prone villages of Badakhshan, Afghanistan. *Int. J. Disaster Risk Reduct.* 33, 5–15. doi:10.1016/j.ijdrr.2018.07.012

Nikolopoulos, E. I., Borga, M., Marra, F., Crema, S., and Marchi, L. (2015). Debris flows in the eastern Italian Alps: Seasonality and atmospheric circulation patterns. *Nat. Hazards Earth Syst. Sci.* 15, 647–656. doi:10.5194/nhess-15-647-2015

Owczarek, P., Opala-Owczarek, M., Rahmonov, O., and Mendecki, M. (2017). 100 years of earthquakes in the Pamir region as recorded in juniper wood: A case study of Tajikistan. *J. Asian Earth Sci.* 138, 173–185. doi:10.1016/j.jseaes.2017.02.011

Picarelli, L., Olivares, L., and Avolio, B. (2008). Zoning for flowslide and debris flow in pyroclastic soils of Campania Region based on "infinite slope" analysis. *Eng. Geol.* 102, 132–141. doi:10.1016/j.enggeo.2008.03.015

Pirulli, M., and Marco, F. (2010). Description and numerical modelling of the october 2000 nora debris flow, northwestern Italian Alps. *Can. Geotechnical J.* 47, 135–146. doi:10.1139/t09-082

Riley, K. L., Bendick, R., Hyde, K. D., and Gabet, E. J. (2013). Frequency-magnitude distribution of debris flows compiled from global data, and comparison with post-fire debris flows in the Western U.S. *Geomorphology* 191, 118–128. doi:10.1016/j.geomorph.2013.03.008

Savi, S., Schildgen, T. F., Tofelde, S., Wittmann, H., Schirler, D., Mey, J., et al. (2016). Climatic controls on debris-flow activity and sediment aggradation: The Del Medio fan, NW Argentina. *J. Geophys. Res. Earth Surf.* 121, 2424–2445. doi:10.1002/2016jf003912

Schoenbohm, L. M., Chen, J., Stutz, J., Sobel, E. R., Thiede, R. C., Kirby, B., et al. (2014). Glacial morphology in the Chinese Pamir: Connections among climate, erosion, topography, lithology and exhumation. *Geomorphology* 221, 1–17. doi:10.1016/j.geomorph.2014.05.023

Shroder, J. F., Weihs, B. J., and Schettler, M. J. (2011). Mass movement in northeast Afghanistan. *Phys. Chem. Earth* 36, 1267–1286. doi:10.1016/j.pce.2011.03.003

Toreti, A., Schneuwly-Bollschweiler, M., Stoffel, M., and Luterbacher, J. (2013). Atmospheric forcing of debris flows in the Southern Swiss Alps. *J. Appl. Meteorology Climatol.* 52, 1554–1560. doi:10.1175/jamc-d-13-077.1

Wang, K., Xiao, W., Windley, B. F., Mao, Q., Ji, W., Sang, M., et al. (2022). The dashui subduction complex in the eastern tianshan-beishan orogen (NW China): Long-lasting subduction-accretion terminated by unique mid-triassic strike-slip juxtaposition of arcs in the southern altaids. *Tectonics* 41, e2021TC007190. doi:10.1029/2021tc007190

Wang, Q., and Zhu, Q. (2013). Razumikhin-Type stability criteria for differential equations with delayed impulses. *Chin. J. Geol.* 48 (1), 1–18. doi:10.14232/ejqtde.2013.1.14

Wang, Z., Wu, H., Zhang, M., Lv, W., and Yang, L. (2020). Distribution and main controlling factors of debris flows in Wuqia county, Xinjiang autonomous region. *Yangtze River* 51 (8), 44–49. doi:10.16232/j.cnki.1001-4179.2020.08.008

Wei, F., Gao, K., Hu, K., Li, Y., and Gardner, J. S. (2008). Relationships between debris flows and Earth surface factors in Southwest China. *Environ. Geol.* 55, 619–627. doi:10.1007/s00254-007-1012-3

Wei, R., Zeng, Q., Davies, T., Yuan, G., Wang, K., Xue, X., et al. (2018). Geohazard cascade and mechanism of large debris flows in Tianmo gully, SE Tibetan Plateau and implications to hazard monitoring. *Eng. Geol.* 233, 172–182. doi:10.1016/j.enggeo.2017.12.013

Wei, Z., Shang, Y., Zhao, Y., Pan, P., and Jiang, Y. (2017). Rainfall threshold for initiation of channelized debris flows in a small catchment based on in-site measurement. *Eng. Geol.* 217, 23–34. doi:10.1016/j.enggeo.2016.12.003

Wieczorek, G. F., Mossa, G. S., and Morgan, B. A. (2004). Regional debris-flow distribution and preliminary risk assessment from severe storm events in the Appalachian Blue Ridge Province, USA. *Landslides* 1, 53–59. doi:10.1007/s10346-003-0003-z

Xiong, J., ChenH.Y.Zeng, L., Su, F. H., Gong, L. F., and Tang, C. X. (2023). Coseismic landslide sediment increased by the "9.5" Luding earthquake, Sichuan, China. *J. Mt. Sci.* 20 (3), 624–636. doi:10.1007/s11629-022-7770-2

You, Y., Wang, D. W., Liu, J. F., Sun, H., Wang, Z., Zhang, W. T., et al. (2023). Assessment of the distribution and hazard tendency of debris flows along the Chengdu-Changdu section of the Sichuan-Tibet traffic corridor. *Bull. Eng. Geol. Environ.* 82 (7), 253. doi:10.1007/s10064-023-03268-3

Yuan, X., Ying, Y., Wei, X., Hou, R., Wang, X., Zhao, Y., et al. (2018). Research status quo and its prevention implication of geological hazards in the Central China Orogen. *Geol. J.* 53 (S1), 252–265. doi:10.1002/gj.3039

Yuan, Z., Chen, J., Owen, L., Hedrick, K. A., Caffee, M. W., Li, W., et al. (2013). Nature and timing of large landslides within an active Orogen, eastern Pamir, China. *Geomorphology* 182, 49–65. doi:10.1016/j.geomorph.2012.10.028

Zhang, M. Z., Xing, A. G., Li, K. Z., Zhuang, Y., Chang, W. B., and Liu, Y. W. (2023). Debris flows in lebai gully along the yarlung tsangpo River in tibet: Characterization, causes, and dynamic prediction of potential debris flows. *Environ. earth Sci.* 82, 25. doi:10.1007/s12665-022-10694-1

Zhang, T. T., Gao, Y., Li, B., Yin, Y. P., Liu, X. J., Gao, H. Y., et al. (2023). Characteristics of rock-ice avalanches and geohazard-chains in the parlung zangbo basin, tibet, China. *Geomorphology* 422, 108549. doi:10.1016/j.geomorph.2022.108549

Zhang, Y., Cheng, Y., Yin, Y., Lan, H., Wang, J., and Fu, X. (2014). High-position debris flow: A long-term active geohazard after the wenchuan earthquake. *Eng. Geol.* 180, 45–54. doi:10.1016/j.enggeo.2014.05.014